Light Trapping effects in Thin Film Silicon Solar Cells.

Journal:	*2009 MRS Spring Meeting*
Manuscript ID:	576929.R1
Symposium:	Symposium A
Date Submitted by the Author:	
Complete List of Authors:	Haug, Franz-Josef; Ecole Polytechnique de Lausanne, Institute of Microengineering Söderström, Thomas; Ecole Polytechnique de Lausanne, Institute of Microengineering Dominé, Didier; SUPSI Ballif, Christophe; Ecole Polytechnique de Lausanne, Institute of Microengineering
Keywords:	photovoltaic, amorphous, thin film

Light trapping effects in thin film silicon solar cells

F.-J. Haug, T. Söderström, D. Dominé, C. Ballif
École Polytechnique Fédérale de Lausanne (EPFL), Institute of Microengineering (IMT),
Photovoltaics and thin film electronics laboratory (PVLab),
Rue A.-L. Breguet 2, 2000 Neuchâtel, Switzerland

ABSTRACT

We present advanced light trapping concepts for thin film silicon solar cells. When an amorphous and a microcrystalline absorber layers are combined into a micromorph tandem cell, light trapping becomes a challenge because it should combine the spectral region from 600 to 750 nm for the amorphous top cell and from 800 to 1100 for the microcrystalline bottom cell. Because light trapping is typically achieved by growing on textured substrates, the effect of interface textures on the material and electric properties has to be taken into account, and importantly, how the surface textures evolve with the thickness of the overgrowing layers. We present different scenarios for the n-i-p configuration on flexible polymer substrates and p-i-n cells on glass substrate, and we present our latest stabilized efficiencies of 9.8% and 11.1%, respectively.

INTRODUCTION

Light scattering at textured interfaces has become a decisive feature for high efficiency thin film silicon solar cells. It allows using thinner absorber layers because the scattering enhances the effective light path in the absorbing film. While this is certainly important for production throughput, light trapping is also mandatory because of inherent material properties; in case of amorphous silicon, the impact of light induced degradation can be reduced in thinner films, in microcrystalline silicon it can, to some extent, compensate the low absorption of the indirect band gap. Light scattering is typically achieved at surface textures of the substrate or of the electric contact layer that precedes the silicon deposition [1]. For superstrate (p-i-n) devices, the transparent front contacts are either directly grown under conditions that favour preferential growth and faceting [2, 3], or they are structured by etching after growth [4]. Similar concepts are followed in substrate (n-i-p) devices for achieving textured metallic back contacts, e.g. the well known surface roughening of silver when it is grown on heated substrates [5]. Typical textures for amorphous silicon solar cells should have a root mean square (rms) surface roughness in the range from 50 to 90 nm, and a lateral feature size which varies between 300 and 500 nm.

For microcrystalline cells, the light trapping range lies between 800 and 1100 nm because of its lower band gap compared to amorphous cells. Empirical data suggest that the lateral feature size should be in the range from 1000 to 1400 nm, while higher rms roughness than in the amorphous case is not necessarily beneficial for the solar cell efficiency [6]. The latter observation might be related to the growth mechanism of microcrystalline silicon which often results in defective material above steep, V-shaped depressions [7, 8].

In micromorph tandem cells, where a microcrystalline and an amorphous absorber are combined in the same device, it becomes a challenging task to devise light scattering strategies that can effectively serve the different spectral ranges of the two individual cells. The first step to achieve this goal is the introduction of an intermediate reflector layer between the two cells, because light trapping in the amorphous top cell is quite simply impossible without reflection of light at its back surface; after its first realization with a thin film of ex-situ ZnO between the cells [9], in-situ solutions with P-doped SiOx have been realized [10], and the intermediate reflector is now established in production of micromorph tandem modules [11].

In this paper, we discuss the possibility of implementing different length scales for light trapping, either in the same interface by overcoating a large structure with smaller features, or by varying the texture between the individual interfaces. This approach must also take into account how a given surface structure evolves during the growth of amorphous and microcrystalline absorber layers, respectively.

EXPERIMENTAL

n-i-p cells

The n-i-p cells presented here are grown on a flexible polyethylene substrate. The surface of the substrate is textured with a periodic sinusoidal structure which is embossed into the surface by a roll-to-roll process [12]. The substrate is covered conformally by sputtering of a bilayer of silver and zinc oxide with thickness of 80 and 60 nm, respectively. The silicon layers are deposited at 180°C by very high frequency plasma enhanced CVD (PE-CVD) from a mixture of silane (SiH_4) and hydrogen (H_2), phosphine (PH_3) and tri-methyl-boron ($B(CH_3)_3$, TMB) are used as doping gases. The front contact consists of a 3.8 µm thick ZnO layer deposited by low pressure CVD (LP-CVD) which results in naturally textured growth [3]. The layer is lightly boron doped in order to suppress free carrier absorption [13]. In the n-i-p tandem cells shown here we use the same LP-CVD process for the deposition of the intermediate ZnO reflector with a thickness of 1.6 µm [14].

p-i-n cells

The p-i-n cells are grown on AF45 borosilicate glass substrates from Schott. First, the substrates are covered with a transparent front contact of LPCVD-ZnO; two different conditions are used, strongly doped films with a thickness of 1.9 µm (type A), and lightly doped films with a thickness of 4.8 µm. The sheet resistance of both substrates is 10 Ω/sq, their surface roughnesses are 66 and 180 nm, respectively. The thicker ZnO layer is subjected to a plasma treatment which changes the initial V-shaped morphology to U-shaped morphology which is better suited for the growth of microcrystalline silicon (type C) [13]. Depending on the duration of the treatment, the roughness can be reduced as much as down to 120 nm [15]. The amorphous and microcrystalline layers are deposited by VHF-PECVD under similar conditions to those of the previous section, but deposition temperatures up 220°C are tested. The intermediate reflector in the presented p-i-n cells is

made from P-doped SiO_x (SOIR) by in-situ processing [10]. The back contact of p-i-n cells consists again of LPCVD-ZnO, covered with a white reflector.

Characterization

The illuminated current voltage characteristics of all cells are measured in standard test conditions (25°C, AM1.5g spectrum, 100 mW/cm^2) with a dual source solar simulator (Wacom). The current density is determined independently by a measurement of the external quantum efficiency (EQE). Red and blue light bias is applied for measuring top- and bottom cells, respectively, and the photocurrent is determined by integration of the EQE weighted by the spectral photon density of the AM1.5g spectrum.

RESULTS AND DISCUSSION

n-i-p cells

As starting consideration for tandem development, we test the realistically attainable total current of the device by studying the dependence of the photocurrent on the bottom cell thickness. Figure 1 presents the EQEs of a series of microcrystalline cells on the 2D grating substrate. When the i-layer thickness increases from 1.1 µm to 2 µm, we observe a large increase in photocurrent from 23 mA/cm^2 to 24.5 mA/cm^2, but for thicker absorber layers the photocurrent tends to saturate at about for i-layers thicker than 2.5 µm. When the thickness is increased further, the electric performance degrades significantly which leads us to the conclusion the saturation reflects a problem with the collection of carriers rather than the limit of light trapping; with improved processing of the microcrystalline i-layer still higher current densities should be possible with our substrate texture.

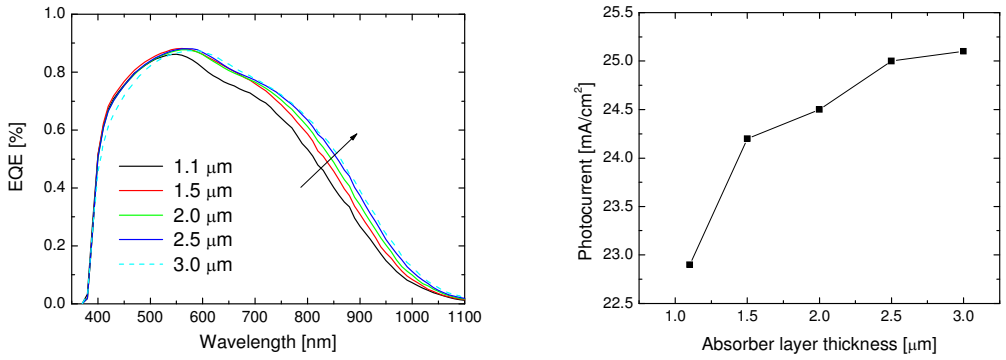

Figure 1: External quantum efficiency of microcrystalline solar cells on the periodic texture (left) and the dependence of photocurrent on the i-layer thickness (right).

Taking a limiting value of the total current of 25 mA/cm^2 for the time being, we can hope to get a matched tandem cell with a current of 12.5 mA/cm^2. However, even this current density is an ambitious goal for the amorphous top cell. If we consider a case where the amorphous top cell is stacked onto the microcrystalline bottom cell without any further enhancement, we can assume no more than one single pass through the

amorphous absorber layer. After passing through the top cell, the remaining light has ample chance to be absorbed in the bottom cell where it can make one passes through a thick absorber layer, undergo diffusion at the back contact and make another pass before it could reach again the amorphous cell. Thus, the top cell in such a tandem does not benefit from the back reflector. The thickness series of top n-i-p amorphous cells in Figure 2 shows that we require an i-layer thickness of more than 600 nm to obtain a photocurrent of more than 12 mA/cm^2. Clearly, such a thickness is not desirable in terms of light induced degradation.

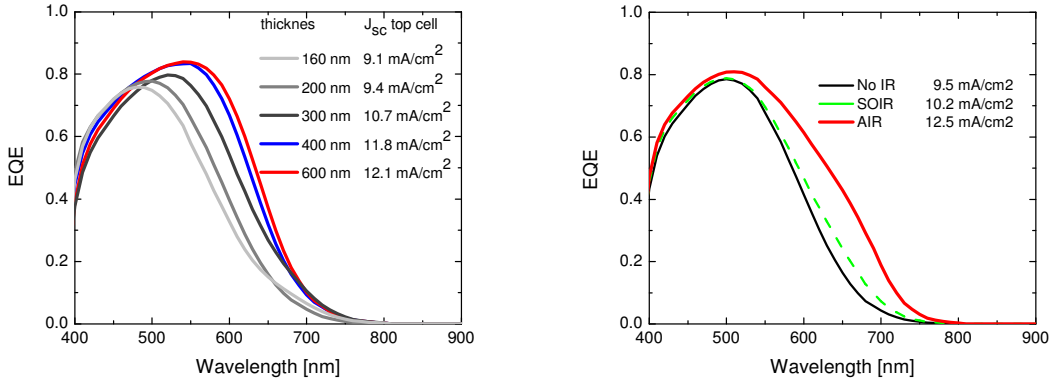

Figure 2: EQEs of the top cell in n-i-p/n-i-p tandem cells on the flexible substrate. The left panel illustrates the variation of i-layer thickness, the right panel illustrates the importance of a textured intermediate reflector layer (i-layer thickness: 200 nm).

By introducing a layer of lower refractive index between the bottom cell and the top cell, we can establish an interference condition where poorly absorbed light in the range between 600 and 750 nm is selectively reflected back into the amorphous absorber layer. The right panel in Figure 2 shows that a 100 nm thick, nominally flat SOIR improves the current in a 200 nm thick top cell from 9.5 mA/cm^2 to 10.2 mA/cm^2.

However, we are still far from the targeted photocurrent of 12.5 mA/cm^2, for two reasons. First, the periodic substrate with its period of 1200 nm is well matched to the requirements of the microcrystalline bottom cells, but not necessarily to amorphous cells. In 270 nm thick single junction amorphous cells deposited directly on this reflector, we obtained photocurrents between 12.8 and 14.4 mA/cm^2 [12], but the reflection at the SOIR in the tandem is very likely to be much inferior to the ZnO/Ag back contact. Second and more importantly, the texture of the back contact is changed by the growth of the microcrystalline bottom cell. Figure 3 shows a cross section image through a tandem cell on the periodic reflector. We observe that the amplitude of the substrate texture is reduced towards the top of the microcrystalline layer, and the sinusoidal shape is changed towards a mostly flat interface with small depressions located along the minima of the initial structure. Thus, the reflection at the SOIR can yield a second pass of light through the top cell, but we expect only little scattering of light at the flattened interface. Correspondingly, the top cell compares well to flat reference cells on a good reflector (e.g. 11 mA/cm^2 for a 270 nm thick cell [16]).

In order to achieve a real light scattering in the top cell, we introduce an asymmetric intermediate reflector (AIR) grown by LPCVD-ZnO [17]. Inherent to the growth process, LPCVD ZnO develops a textured surface regardless whether the

substrate is flat or mildly textured, and it is well documented that this surface texture is well adapted to amorphous solar cells [18]. Figure 3 shows that a 1.6 µm thick LPCVD-ZnO layer completely fills the small depressions in the surface of the microcrystalline layer, and develops its own typical pyramidal texture independent of the original periodicity.

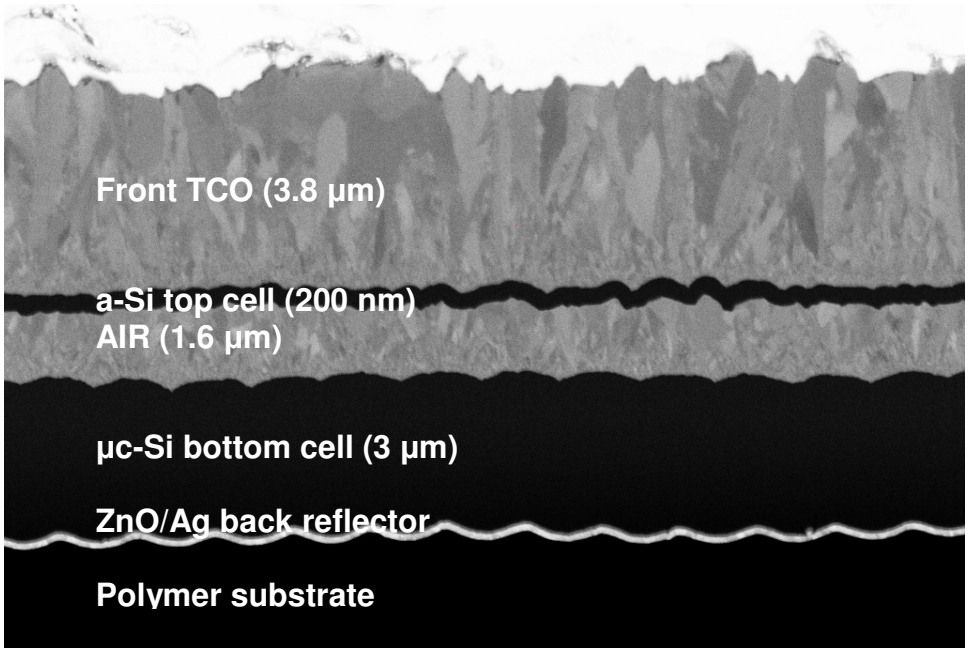

Figure 3: Cross section image through a micromorph tandem cell with LPCVD-ZnO AIR on the periodically textured polymer substrate.

Figure 2 shows that the asymmetric intermediate reflector results in a massive improvement of the top cell current, indeed, we achieve the goal of 12.5 mA/cm^2 in a 200 nm thick amorphous cell. The best cell of the AIR development showed an initial efficiency of 11.2%. After 1000 h of light soak, the efficiency stabilized at 9.8%.

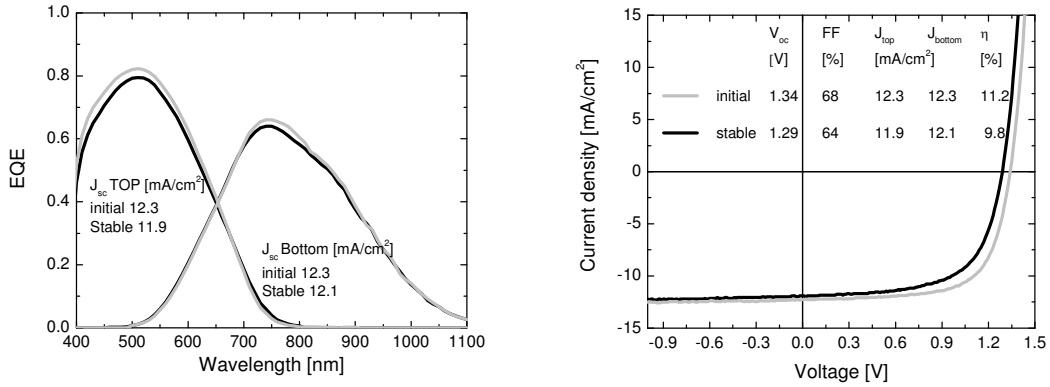

Figure 4: External quantum efficiency (left) and current voltage characteristic (right) of micromorph tandem cells with AIR on flexible polymer substrate in initial and stabilized state (1000 h light soak at 50°C and an illumination density of 100 mW/cm^2)

p-i-n cells

The p-i-n cell development is carried out on glass substrates covered with an LPCVD-ZnO front contact. Figure 5 shows typical surface morphologies for type A and type C substrates. Type A substrates consist of randomly distributed pyramids with a typical lateral feature size of 300 nm and clearly defined facets, whereas the surface treated type C substrates consist of large features (about 800 to 1000 nm) with rounded out bottoms of U-shape.

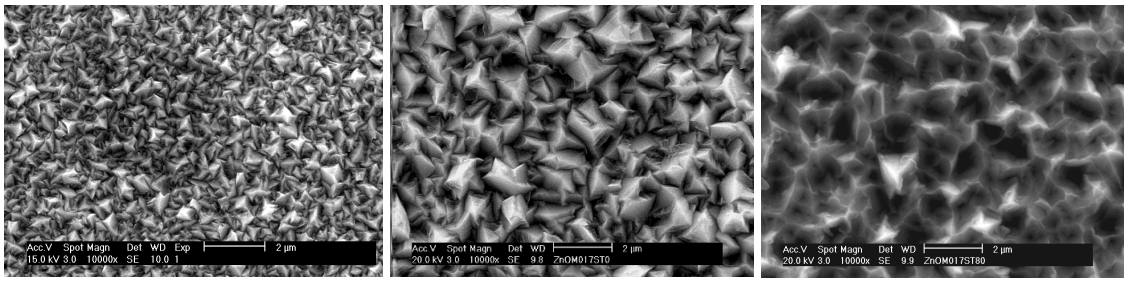

Figure 5: Surface morphology of type A substrate (left). Thicker films show similar shape, but bigger features (middle). A surface treatment yields type C substrate (right).

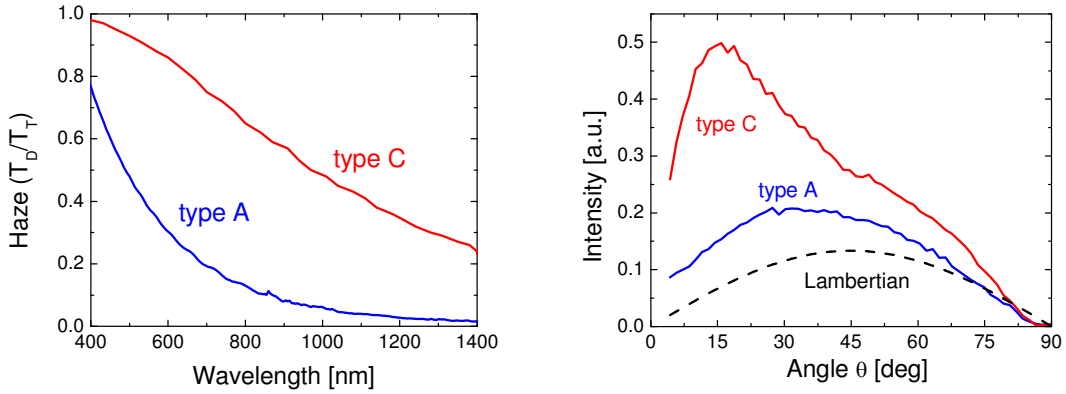

Figure 6: Spectral haze of type A and type C substrates (left panel). The right panel shows the sin-weighted ARS, the dotted line illustrates ideal Lambertian scattering.

Figure 6 compares the optical characteristics of the two layers; the haze is defined as ratio of diffuse to total transmission $H=T_D/T_T$, the angle resolved scattering (ARS) is the intensity scattered into angles between 0 and 90° for a fixed wavelength. For randomly rough surfaces with a correlation length much smaller than the wavelength, scalar scattering theory predicts the following relation between haze and wavelength [19, 20].

$$H = 1 - \exp\left\{-\left(\frac{2\pi\sigma}{\lambda}\left|n_1\cos\theta_1 - n_2\cos\theta_2\right|\right)^{\beta}\right\}$$

The angles θ_1 and θ_2 represent the incident beam and the direction of the scattered beam, respectively; n_1 and n_2 are the corresponding refractive indices. The exponent β

should be equal to 2, but different values have been reported experimentally [20, 21]. The haze data are shown in the left panel of Figure 6; we find β values of 2.8 and 2 for the type A substrate and the type C substrate, respectively [22]. The ARS data in the right panel are plotted after weighting with the sinus of the scattered angle which provides the shape of the probability density function associated to the angular distribution. The type A substrate shows a maximum a 40° which is very close to the behaviour of an ideal Lambertian diffuser (maximum at 45°), indicating that it scatters effectively into high angles. The type C substrate scatters into a narrow angular distribution, the most probable scattering angle being only 20°. Assuming rotational symmetry with respect to surface normal (ARS not dependent on the polar angle φ), the integrated areas under the curves are proportional to the diffuse part of the transmittance T_D. Their variation reflects the different haze values for the wavelength of the ARS measurement, in this case at 543 nm.

$$T_D \sim \iint ARS \cdot \sin\theta \cdot \mathrm{d}\varphi\,\mathrm{d}\theta = 2\pi \cdot \int ARS \cdot \sin\theta \cdot \mathrm{d}\theta$$

Figure 7 compares EQEs of tandem cells on the two different types of LPCVD ZnO front contacts; the top and bottom cell thicknesses are 290 nm and 3.0 µm, respectively. The cells without intermediate reflector in the left panel show identical top cell currents of 10.9 mA/cm^2, but the moderately doped type C substrate yields better bottom currents because of the lower free carrier absorption in the TCO and because the large grained type C structure is better suited for light trapping in the bottom cell. The behaviour of the EQEs in the top cells suggests that the current is essentially produced in one single pass through the amorphous absorber. The right panel shows the situation after the introduction of a SOIR with 150 nm thickness. Both top amorphous cells gain in current because of reflection at the SOIR, but we observe a larger gain in the device with the type A front contact (2.6 mA/cm^2 compared to 2.1 mA/cm^2 on the type C substrate). We can understand the observations in terms of the optical measurements shown in Figure 6 when we assume that, when multiple reflections can occur within the top cell, the broad ARS of the type A substrate can offset its lower haze values. We have to keep in mind though, that the optical measurements in air are different from the situation in the cell where the actual scattering interface is between ZnO and silicon, not between ZnO and air.

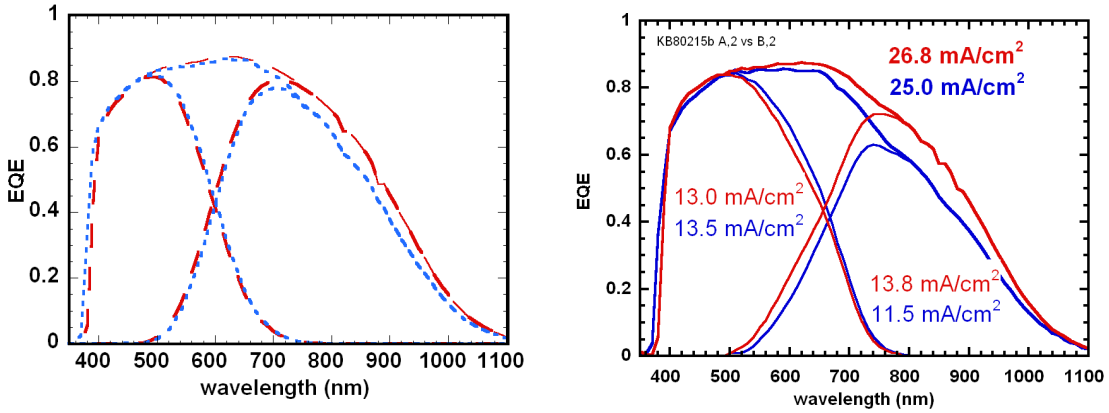

Figure 7: External quantum efficiencies of tandem solar cells on type A and type C substrates; left: no SOIR, right: with 150 nm thick SOIR.

We tried to combine the beneficial scattering effects of both types of substrates in a dedicated experiment by growing ZnO of type A on top of a substrate similar to type C. With this approach we intended to supply small features of type A for light scattering into the top cell. Furthermore, we anticipate that the flattening of the small features during the growth of the amorphous absorber should still maintain the larger features for scattering into the bottom cell. We compare a set of four different substrates including a type C substrate as reference (sample D3). The A3 sample is similar to the type C, but thinner; consequently it shows smaller features. The details of the substrate fabrication sequence are given in Table 1, further details can be found in [23].

Table 1: Design of the substrates for the double layer test

	A3	B3	C3	D3
Thickness 1st layer (µm)	3.6	3.6	3.6	4.5
SiOx layer		yes	no	
Thickness 2nd layer (µm)	-	1.1	1.1	
σ_{rms} (nm)	100	102	152	159
Comment:	"thin" type C	Figure 8 right	Figure 8 left	type C

The samples B3 and C3 are double structures, but care must be taken because the two constituent layers are made from the same material, ZnO. Thus, it turned out that simple stacking with surface treatment in-between just resumes the growth of the large grained ZnO in a form of local epitaxy, resulting in the formation of preferred surface facets very similar to the type C substrate before the surface treatment (c.f. left panel of Figure 8 compared to middle panel of Figure 5). The insertion of a thin SiOx layer using the same conditions as the SOIR layer, but only 5 nm thick, can effectively break the local epitaxy and force the ZnO to nucleate new grains. The right panel of Figure 8 shows that the result is a double structure that resembles to some extent the recently developed Asahi W structure [24].

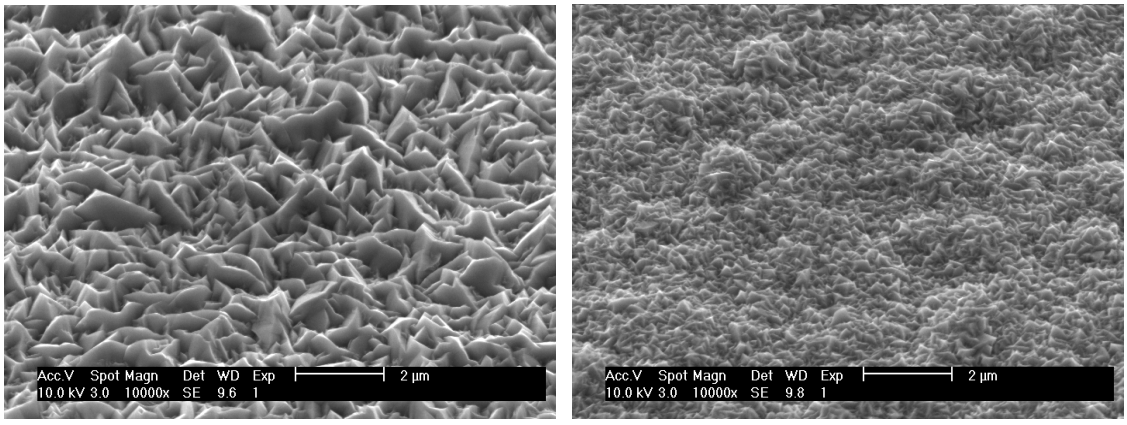

Figure 8: Stacking of type A ZnO on type C ZnO. In the left panel no interface treatment was used resulting in resumed grain growth and large features (sample C3), in the right panel a thin layer of SiOx was inserted, breaking the grain growth (sample B3).

Figure 9 compares the ARS of the four different substrates listed in Table 1. As expected, the single layer samples A3 and D3 are similar; their behaviour in the shallow angle range is identical, but we observe that D3 shows more scattering into large angles. The double structure without the SiOx treatment (sample C3) shows the best scattering into high angles, resembling in fact the type A structure of Figure 6. Surprisingly, the sample B3 with its clearly distinguishable double structure shows very poor scattering into high angles, but strong contributions into small angles around ~15°.

The EQEs of tandem cells with SOIR on the four different samples are shown in the right panel of Figure 9. We observe that the sample B3 shows poor light trapping in the bottom cell for wavelengths greater than 750nm, while the EQEs of the other samples are identical in this range. In the visible range between 550 and 700 nm, the inset shows that the top cell EQEs are higher in the double structures (samples B3 and C3) than in the single structures (samples A3 and D3). In the same range, the bottom EQEs of samples B3 and C3 are lower, indicating an efficient redistribution of light into the top cell. At this stage of development, it appears that among the double structures the configuration of sample C3 is preferable to B3, even though on that sample the character of a double structure is not obvious from Figure 8.

The poor performance of the B3 sample could possibly be explained by the poor ARS of this sample, but for the other substrates in this test the correspondence is much less evident. We should keep in mind that the measurement in air does not necessarily reflect the real light scattering properties in the cell. Recently, we proposed an optical model based on a Fourier approach [25] which is capable of predicting the behaviour of the ARS on the basis of AFM surface profile data [23]. We are confident that this tool will be useful in our further development of double structures because the calculations can be benchmarked against measured ARS data, and they can more reliably predict the behaviour in solar cells using realistic refractive indices.

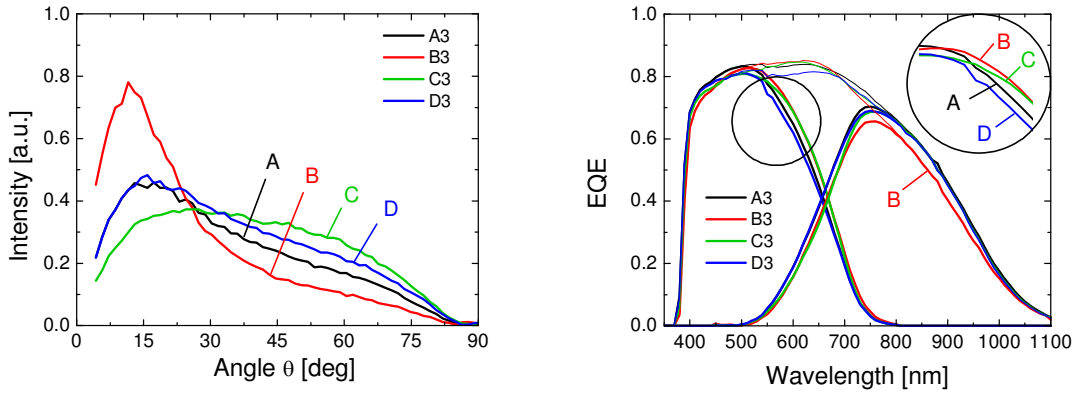

Figure 9: Comparison sin-weighted ARS data of a double layer test (left panel, layer types explained in text). The right panel shows the EQEs of tandem solar cells with SOIR on the different structures, the inset gives the details of the top cell EQEs.

After this brief outlook on new, but not yet fully conclusive double structures, we conclude this section on p-i-n tandem solar cells by reverting to the type C substrate; Figure 10 shows data on the electric performance of a configuration combining a top cell thickness of 300 nm, a bottom cell thickness of 3µm, and a SiOx intermediate reflector

layer of 150 nm thickness. In this configuration, and without anti-reflection coating, we obtain an initial efficiency of 12.6% which shows a relative degradation of 12% after 1000 h of light soaking, reaching a stabilized efficiency of at 11.1%. The area of this cell is 1.2 cm^2.

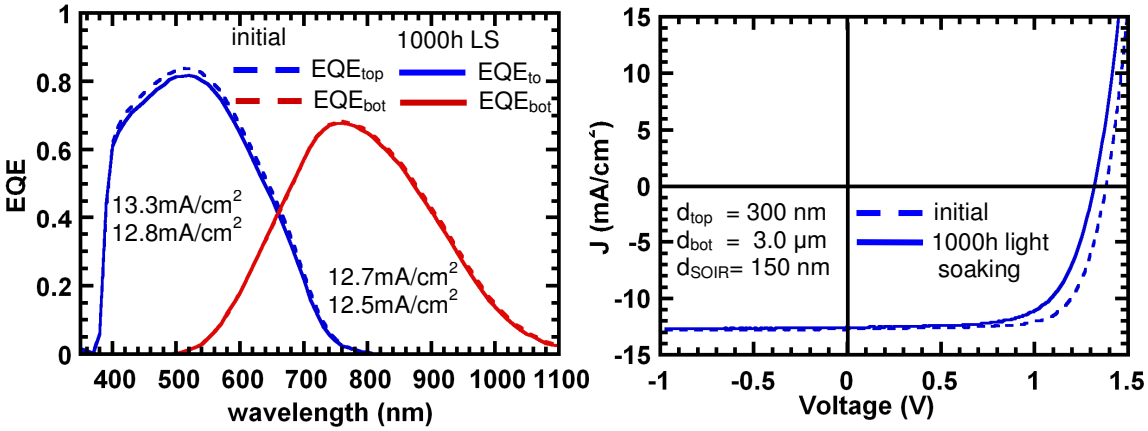

Figure 10: EQE and current voltage characteristics of a micromorph tandem solar cell with SOIR on the type C substrate in its initial and stabilized state (cell size 1.2 cm^2, no anti-reflection coating).

CONCLUSIONS

We presented thin film silicon tandem cells in n-i-p and p-i-n configuration. High efficiencies necessitate matched current densities higher than 12.5 mA/cm^2, but at the same time their thickness should not exceed 300 nm in order to avoid light induced degradation. Currently, an intermediate reflector between the top and bottom cells is the most successful route towards high top cell current densities. In n-i-p tandems, we observed that growth of the thick bottom cell results in adverse changes of the surface morphology, resulting in an almost flat interface. The potential of the intermediate reflector is very limited in these circumstances. By introducing surface texture into the intermediate reflector layer itself, we were able to supply to the top cell its very own light scattering interface, and we are at liberty to use a structure that is experimentally well proven for this purpose. We are able, on plastic substrate to apply that scheme to reach close to 10% stable efficiency micromorph cell, with an initial matched current of 12.3 mA/cm2 . We tried to apply the same line of arguments to the related case of p-i-n cells; a structure that combines small and large features should provide the fine features for light diffusion in the top cell while the flattening effect of growing the amorphous layer should not affect too seriously large features which could then diffuse longer wavelengths for light trapping in the bottom cell. We could successfully fabricate ZnO surfaces that show textures on two different length scales, but so far their application into tandem solar cells did not show a clear improvement. Single structure large grain TCO still leads to the best stable efficiencies over 11% with 12.5 mA/cm2 current.

ACKNOWLEDGEMENTS

Funding by the EU projects Flexcellence (contract No. 019948) and Athlet (contract No. 019670) as well as support from the Swiss Federal Office for Energy (OFEN) under project No. 101191 are thankfully acknowledged.

REFERENCES

1. H. W. Deckman, C. R. Wronski, H. Witzke, and E. Yablonovitch, *Optically Enhanced Amorphous-Silicon Solar-Cells.* Applied Physics Letters, 1983. **42**(11): p. 968-970.
2. M. Kambe, M. Fukawa, N. Taneda, Y. Yoshikawa, K. Sato, K. Ohki, S. Hiza, A. Yamada, and M. Konagai. *Improvement of light-trapping effect on microcrystalline silicon solar cells by using high haze transparent conductive oxide films*. in *Proc. 3rd World PVSEC*. 2003. Osaka. p. 1812-1815
3. S. Fay, J. Steinhauser, N. Oliveira, E. Vallat-Sauvain, and C. Ballif, *Opto-electronic properties of rough LP-CVD ZnO:B for use as TCO in thin-film silicon solar cells.* Thin Solid Films, 2007. **515**(24): p. 8558-8561.
4. O. Kluth, B. Rech, L. Houben, S. Wieder, G. Schöpe, C. Beneking, H. Wagner, A. Löffl, and H. W. Schock, *Texture etched ZnO: Al coated glass substrates for silicon based thin film solar cells.* Thin Solid Films, 1999. **351**(1-2): p. 247-253.
5. A. Banerjee and S. Guha, *Study of Back Reflectors for Amorphous-Silicon Alloy Solar-Cell Application.* Journal of Applied Physics, 1991. **69**(2): p. 1030-1035.
6. R. Franken, R. Stolk, H. Li, C. van der Werf, J. Rath, and R. Schropp, *Understanding light trapping by light scattering textured back electrodes in thin film n-i-p-type silicon solar cells.* Journal of Applied Physics, 2007. **102**: p. 014503.
7. M. Python, E. Vallat-Sauvain, J. Bailat, D. Dominé, L. Fesquet, A. Shah, and C. Ballif, *Relation between substrate surface morphology and microcrystalline silicon solar cell performance.* Journal of Non-Crystalline Solids, 2008. **354**(19-25): p. 2258-2262.
8. H. Li, R. Franken, J. Rath, and R. Schropp, *Structural defects caused by a rough substrate and their influence on the performance of hydrogenated nano-crystalline silicon n–i–p solar cells.* Solar Energy Materials and Solar Cells, 2009.
9. D. Fischer, S. Dubail, J. D. Anna Selvan, N. Pellaton Vaucher, R. Platz, C. Hof, U. Kroll, J. Meier, P. Torres, H. Keppner, N. Wyrsch, M. Goetz, A. Shah, and K.-D. Ufert. *The micromorph solar cell: extending a a-Si:H technology twoards thin film crystallline silicon*. in *Proc. 25th IEEE PVSC*. 1996. Washington D. C. p. 1053-1056
10. P. Buehlmann, J. Bailat, D. Domine, A. Billet, F. Meillaud, A. Feltrin, and C. Ballif, *In situ silicon oxide based intermediate reflector for thin-film silicon micromorph solar cells.* Applied Physics Letters, 2007. **91**(14): p. 143505.
11. K. Yamamoto, A. Nakajima, M. Yoshimi, T. Sawada, S. Fukuda, T. Suezaki, M. Ichikawa, Y. Koi, M. Goto, and T. Meguro, *A high efficiency thin film silicon solar cell and module.* Solar Energy, 2004. **77**(6): p. 939-949.

12. F.-J. Haug, T. Söderström, M. Python, V. Terrazzoni-Daudrix, X. Niquille, and C. Ballif, *Development of micromorph tandem solar cells on flexible low cost plastic substrates.* To be published in Sol. En. Mat., 2009.
13. J. Bailat, D. Dominé, R. Schlüchter, J. Steinhauser, S. Faÿ, F. Freitas, C. Bücher, L. Feitknecht, X. Niquille, R. Tscharner, A. Shah, and C. Ballif. *High efficiency pin microcrystalline and micromorph thin film silicon solar cells deposited on LPCVD ZnO coated glass substrates*. in *Proc. 4th World PVSEC*. 2006. Hawaii. p. 1533-1536
14. T. Söderström, F. J. Haug, X. Niquille, V. Terrazoni-Daudrix, and C. Ballif, *Asymmetrid intermediate reflector for tandem micromorph thin film silicon solar cells.* Applied Physics Letters, 2009. **94**: p. 063501.
15. D. Dominé, P. Buehlmann, J. Bailat, A. Billet, A. Feltrin, and C. Ballif. *High-efficiency micromorph silicon solar cells with in-situ intermediate reflector depositd on various rough LPCVD-ZnO*. in *Proc. 23rd European PVSEC* 2008. Valencia. p. 2091-2095
16. T. Söderström, F. J. Haug, V. Terrazzoni-Daudrix, and C. Ballif, *Optimization of amorphous silicon thin film solar cells for flexible photovoltaics.* Journal of Applied Physics, 2008. **103**(11): p. 114509-114509.
17. T. Söderström, *Single and multi-junction thin film silicon solar cells for flexible photovoltaics*, PhD Thesis, University of Neuchatel, 2009
18. J. Meier, J. Spitznagel, U. Kroll, C. Bucher, S. Faÿ, T. Moriarty, and A. Shah, *Potential of amorphous and microcrystalline silicon solar cells.* Thin Solid Films, 2004. **451**: p. 518-524.
19. C. K. Carniglia, *Scalar scattering theory for multilayer optical coatings.* Optical Engineering, 1979. **18**(2): p. 104–115.
20. M. Zeman, R. Van Swaaij, J. W. Metselaar, and R. E. I. Schropp, *Optical modeling of a-Si: H solar cells with rough interfaces: Effect of back contact and interface roughness.* Journal of Applied Physics, 2000. **88**: p. 6436.
21. H. Stiebig, T. Brammer, T. Repmann, O. Kluth, N. Senoussaoui, A. Lambertz, and H. Wagner. *Light Scattering in Microcrystalline Silicon Thin Film Solar Cells*. in *Proc. 16th EU-PVSEC*. 2000. Glasgow. p. 549-552
22. D. Domine, P. Buehlmann, J. Bailat, A. Billet, A. Feltrin, and C. Ballif, *Optical management in high-efficiency thin-film silicon micromorph solar cells with a silicon oxide based intermediate reflector.* Physica Status Solidi (RRL)-Rapid Research Letters, 2008. **2**(4).
23. D. Domine, *The role of front electrodes and intermediate reflectors in the optoelectronic properties of high-efficiency micromorph solar cells*, PhD Thesis, University of Neuchatel, 2009
24. T. Oyama, M. Kambe, N. Taneda, and K. Masumo. *Requirements for TCO substrate in Si-based thin film solar cells - toward tandem*. in *MRS Spring Meeting*. 2008. San Francisco. p. KK02-01
25. J. E. Harvey and A. Krywonos. *A Global View of Diffraction: Revisited*. in *Proc. SPIE AM100-26*. 2004. Denver. p.